Results of the search for an A boson decaying to Zh, with an $\ell\ell\tau\tau$ final state, in pp collisions at 8 TeV centre of mass energy recorded with the ATLAS experiment

Guillermo Nicolas Hamity

1 Jan Smuts Avenue, Braamfontein, Johannesburg, 2000, South Africa

E-mail: guillermo.nicolas.hamity@cern.ch

Abstract. The neutral CP-dd boson A is predicted by many models with an extended Higgs sector. Searching for the A boson in the sensitive Zh decay, where h is assumed to be the LHC discovered Higgs boson, within the mass range of $220 - 1000$ GeV, offers a gateway to find physics beyond the Standard Model. A search for a gluon-fusion-produced A in the decay to Zh, with a final state of two light leptons and two tau leptons, is conducted with 20.3 fb^{-1}of proton-proton collision data at 8 TeV center of mass energy. The data driven background estimations, background reduction techniques and systematic uncertainty calculations are presented. Upper limits on the cross section times branching ratio of the A boson decaying to $\ell\ell\tau\tau$ are set for various 2-Higgs-Doublet-Model (2HDM) scenarios. Where no excess is observed, exclusion limits are set on ranges of the 2HDM phase-space.

1. Introduction

The Standard Model (SM) is the centrepiece describing the underlying principles of fundamental particle interactions at high energies. The model combines the fundamental electromagnetic, weak and strong forces, and is able to predict known particle interactions with great precision. The SM has withstood the test of multiple experimental observations, with it's *tour de force* being the recent discovery of the Higgs boson which is predicted in the SM by the ATLAS and CMS experiments at the LHC in Geneva [1, 2]. The discovered Higgs boson was found with a mass around 125 GeV and is thus far consistent with the SM zero-spin and positive-parity hypothesis [3, 4]. It therefore comes as no surprise that present ambiguities with the SM are not phenomenological, but stem rather from the it's 'collage-type' derivation [5]. The repetition of fermionic families and the un-quantification of quark charges suggest that the SM may be a low energy state of some underlying theory. More troublesome is that the SM gives no cause for the imbalance of matter over anti-matter, and excludes the gravitational force and dark matter. Models that describe Beyond the Standard Model (BSM) physics are generally aimed at answering some of these questions. In this light, searching for inconsistencies in the SM is crucial to searching for BSM phenomena.

One of the most basic extensions to the SM is by including an additional Higgs doublet in it's derivation [6]. The SM Higgs sector is only comprised of a simple scalar structure. When considering that the fermionic structure has multiple families and mixings, this assumption

need no be the case. The extended models with two Higgs doublets are intuitively referred to as 2-Higgs-Doublet-Models (2HDMs). They include the Minimal Supersymmetric Standard Model (MSSM), an important candidate of Supersymmetry (SUSY), as well as axion [7] and baryogenesis [8] models. After including an additional Higgs doublet, as well as a few intuitive assumptions [6], 2HDMs give rise to five 'Higgs' bosons. There are two CP-even bosons, the light h and heavy H, distinguishable only by their mass, where $m_h < m_H$. Then there are two charged Higgs bosons, denoted as $H^{\pm}$, and a single CP-odd pseudoscalar, the A boson. One should note that the h and H bosons are candidates for the discovered boson, due to their zero-charge and even-parity nature. This allows for 2HDM searches where the mass of one of the CP-even bosons is that of the discovered Higgs. Generally in 2HDM searches one assumes that $m_h = 125$ GeV, although it is still feasible that the light Higgs lives somewhere in the $m_h < 125$ GeV range. Another common assumption made is that the remaining Higgs bosons have approximately equal masses $m_A \approx m_{H^{\pm}} \approx m_H$ [9]. With these assumptions the 2HDM phasespace is reduced considerably to three free parameters: the mass of one of the heavier Higgs bosons (*e.g* m_A), the mixing angle of the two CP-even Higgs bosons, α, and the ratio of the vacuum expectation values of the two Higgs doublets, β. The last two parameters are generally represented as $\tan\beta$ and $\cos(\beta-\alpha)$ for convenience. In direct searches for the 2HDM bosons, all thee parameters are allowed to vary. Furthermore the predicted couplings of the bosons to the vector bosons and fermions fluctuate in terms of $\tan\beta$ and $\cos(\beta-\alpha)$. An additional freedom in terms of the way that each Higgs doublet couples to vector bosons and fermions gives rise to four different 2HDM types. The ratio of the predicted coupling scale factors for the different 2HDM scenarios of the h boson to the SM Higgs boson couplings is given in table 1. Coupling ratios to the vector bosons (κ_V), up-type quarks (κ_u), down-type quark (κ_d), and leptons (κ_ℓ) are shown to vary as functions of β and α.

Table 1. Ratio of predicted coupling scale factors to SM particles of the four 2HDM h bosons to the predicted SM Higgs couplings [13].

Coupling scale factor	Type-I	Type-II	Type-III	Type-IV
κ_V	$\sin(\beta-\alpha)$	$\sin(\beta-\alpha)$	$\sin(\beta-\alpha)$	$\sin(\beta-\alpha)$
κ_u	$\cos(\beta)/\sin(\alpha)$	$\cos(\beta)/\sin(\alpha)$	$\cos(\beta)/\sin(\alpha)$	$\cos(\beta)/\sin(\alpha)$
κ_d	$\cos(\beta)/\sin(\alpha)$	$-\sin(\alpha)/\cos(\beta)$	$\cos(\beta)/\sin(\alpha)$	$-\sin(\alpha)/\cos(\beta)$
κ_ℓ	$\cos(\beta)/\sin(\alpha)$	$-\sin(\alpha)/\cos(\beta)$	$-\sin(\alpha)/\cos(\beta)$	$-\sin(\alpha)/\cos(\beta)$

Direct searches for 2HDM boson set upper limits on the cross section times decay branching ratio of a specific final state channel. In this way we are able to search for the existence of the 2HDM bosons and subsequent traces of BSM physics. As a bi-product of these studies one is able to exclude the existence of 2HDMs from certain areas of the m_A, $\tan\beta$, and $\cos(\beta-\alpha)$ phasespace if no sufficient excess above the upper limits is observed. Various searches have already been conducted, including the CMS searches for $H \to hh$ and $A \to Zh$ between $260-360$ GeV [10], and an independent search for $A \to Zh \to \ell\ell b\bar{b}$ [11]; and the $A \to \tau\tau$ search with ATLAS [12]. No excess was measured in the studies and large sections of the 2HDM phasespace were excluded. Indirect exclusion limits have also been placed on 2HDMs in the ($\tan\beta$, $\cos(\beta-\alpha)$) plane by interpreting the observed couplings of the discovered Higgs boson to other particles [13]. The ($\tan\beta$, $\cos(\beta-\alpha)$) phasespace is scanned for points where the measured Higgs couplings disagree with the 2HDM predictions, at 95% CL or greater, so as to exclude regions in ($\tan\beta$, $\cos(\beta-\alpha)$). There are however areas of phasepace for 2HDMs which have not been probed due to the low branching ratios of the various topologies.

The $A \to Zh$ channel with the h decaying to $\tau\tau$ and Z to $\ell\ell$ is a new search that promises good sensitivity. In particular this channel probes areas of the Type-II and Type-IV 2HDMs which have not been accessible in previous searches. In this topology three orthogonal final states are available, depending on the either leptonic or hadronic decay of each tau lepton. They are $\tau_{lep}\tau_{lep}$, $\tau_{lep}\tau_{had}$ and $\tau_{had}\tau_{had}$. The production of the pseudoscalar A boson is predominantly driven by gluon-fusion. Contributions from b-associated production only become relevant for Type-II and Type-IV 2HDMs at high values of $\tan\beta$, dominating over gluon-fusion at around $\tan\beta = 10$ [9]. In most cases the ratio of b-associated A boson production to that of gluon-fusion is restricted to $< 3\%$. Two leading order Feynman diagrams of the gluon-fusion and b-associated A productions are shown in figure 1.

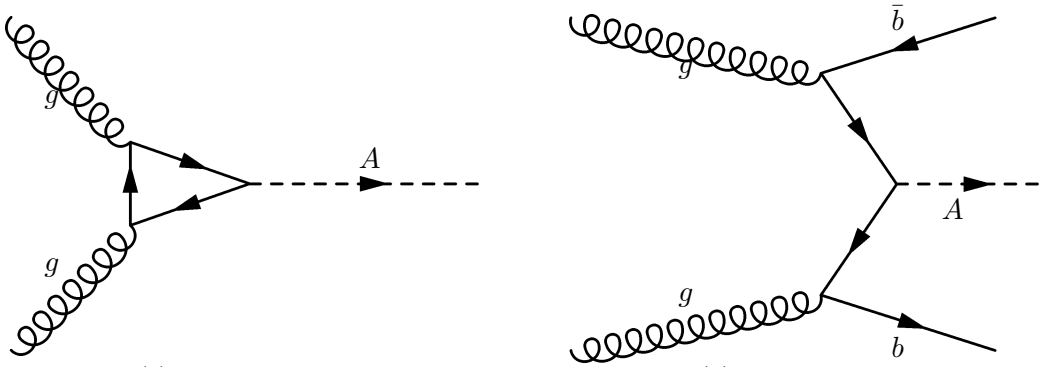

(a) gluon-fusion (b) b-associated

Figure 1. Feynman diagrams for (a) gluon-fusion and (b) b-associated A boson production.

Generally speaking, $A \to Zh$ is the dominant decay mode of A in any 2HDM when the mass of the A is less than two times the mass of the top-quark ($m_h + m_Z < m_A < 2m_t$). This makes the $A \to Zh$ channel a very promising search. At masses of $m_A > 2m_t$ the branching ratio BR($A \to Zh$) drops drastically due to the exposed $t\bar{t}$ kinematic region. In this paper the results from the search of the gluon-produced A boson decaying to $Zh \to \ell\ell\tau_{had}\tau_{had}$ are presented in the range of $220 < m_A < 1000$ GeV. The results are combined with the $\tau_{lep}\tau_{lep}$ and $\tau_{lep}\tau_{had}$ searches and finally interpreted in the various 2HDM scenarios in conjunction with a complementary $A \to Zh \to ffb\bar{b}$ analysis, where $f = \ell,$ or ν.

2. The ATLAS detector

The LHC is currently the largest man-made particle accelerator in the world, capable of proton-proton (pp), and heavy ion (lead-proton (Pb-p) and lead-lead (Pb-Pb)) collisions. It has a circumference of 27 km, a design center-of-mass energy of 14 TeV, and peak instantaneous luminosity of 10^{34} cm^{-2}s^{-1} for pp collisions. The ATLAS detector is one of the two general-purpose detectors at the LHC [14]. It was designed to accommodate a wide spectrum of different physics signatures and explore processes stemming from the TeV mass scale, where groundbreaking discoveries are expected. The ATLAS detector is a multi-purpose particle detector with approximately forward-backward symmetric cylindrical geometry. ATLAS uses a right handed coordinate system with the origin at the interaction point. The z-axis is along the beam pipe, x-axis points towards the center of the LHC ring and the y-axis points up. Polar coordinates (r, ϕ) are used in the transverse plane, ϕ being the azimuthal angle around the beam pipe. The pseudorapidity η is defined as $\eta = -\ln(\tan(\theta/2))$ where θ is the angle between the particle momentum 3-vector and the beam axis. The inner detector (ID) covers $|\eta| < 2.5$ and consists of silicon pixels, silicon micro-strips and a transition radiation tracker. The ID is surrounded by a superconducting solenoid providing a 2 T magnetic field. Surrounding the

ID are two calorimeters, the inner electromagnetic (EM) and the outer hadron calorimeters. The EM calorimeter measures the energy and the position of EM showers within $|\eta| < 3.2$ as well as hadronic showers in the end-cap ($1.5 < |\eta| < 3.2$) and forward ($3.1 < |\eta| < 4.9$) regions. The hadronic calorimeter measures hadronic showers in the central region ($|\eta| < 1.7$). The muon spectrometer surrounds the calorimeters and consists of three subsystems: eight superconducting air-core toroid magnets, a system of tracking chambers and a fast tracking chamber for triggering. A three-level trigger system selects events to be recorded for offline analysis.

3. The $A \to Zh \to \ell\ell\tau_{had}\tau_{had}$ analysis

A search for $A \to Zh(\tau\tau)$ is conducted with the 2012 ATLAS data at 8 TeV, where the light h boson is assumed to have a mass of $m_h = 125$ GeV. Signal Monte Carlo (MC) samples are produced with Pythia8 [15] for A masses at fixed working points: $m_A =$ 220, 240, 260, 300, 340, 350, 400, 500, 800, 1000 GeV. As mentioned in the introduction, each tau in the analysis can decay leptonically (35%) or hadronically (65%). Since tau leptons are massive particles, they decay quickly in the detector and are never observed directly in ATLAS, but can only be reconstructed from their decay products. This makes differentiating light-leptons stemming from leptonic-tau-decays to light-leptons stemming from other processes virtually impossible. As such, tau leptons in the ATLAS detector are considered to be hadronically decaying taus. Tau leptons decay hadronically into either 1− or 3−charged pions, with a ν_τ and possibly a neutral pion. Since the BR($A \to Zh$) is already relatively small, and since the SM branching ratio BR($h \to \tau\tau$) is around 1000 times larger that BR($h \to \mu\mu$), searches in the $\tau_{lep}\tau_{lep}$ and $\tau_{lep}\tau_{had}$ channels can be conducted in $\tau\tau$ without worrying about contamination from $h \to \ell\ell$ ($\ell \neq \tau$). In all three analysis stradegies, the reconstructed A boson mass, m_A, is considered as the parameter of interest.

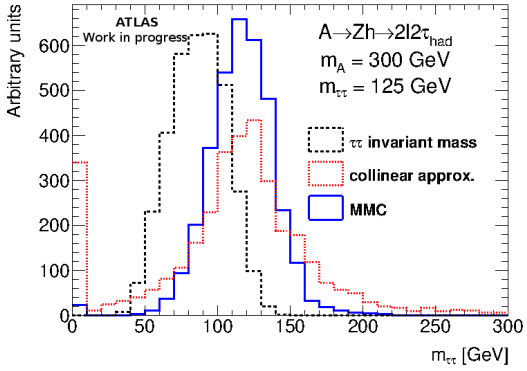

Figure 2. Comparison of $m_{\tau\tau}$ distributions of a $m_A = 300$ GeV MC signal sample decaying via $\tau_{had}\tau_{had}$ using different di-tau mass reconstruction techniques.

The fully hadronic final state is a particularly challenging analysis since it contains a large amount of missing transverse energy, E_T^{miss}, from the two neutrinos. In the case of $\tau_{had}\tau_{had}$, full reconstruction of the event topology requires solving a system of equations with 6 unknowns. This system is under-constrained and an exact solution is not possible. Therefore, the full event reconstruction, as well as the full reconstruction of the $m_{\tau\tau}$ mass, are impossible. The Missing Mass Calculator (MMC) method is therefore used to reconstruct $m_{\tau\tau}$ [16]. This method scans for the most likely $m_{\tau\tau}$ solution given the known conditions of the event, *i.e.* the visible taus and E_T^{miss} kinematics. Figure 2 shows the performance of the MMC for $m_{\tau\tau}$ of the $\tau_{had}\tau_{had}$ MC

signal. The MMC is compared to alternate $m_{\tau\tau}$ reconstruction methods: the transverse mass and collinear approximation (CLA) methods [16]. The MMC gives a mass around 125 GeV as expected, performing at a better efficiency and resolution than the CLA method.

The event selection in the $\tau_{had}\tau_{had}$ channel focuses on selecting a clean signal with exactly two leptons (e, or μ) and two visible tau jets. Events are triggered by single lepton triggers. The events are required to have exactly two same flavour opposite charge loose leptons with a combined invariant mass of $80 < m_{\ell\ell} < 100$ GeV, which corresponds to $m_Z = 90$ GeV. Track and calorimeter track isolation requirements are also imposed on the leptons. The event must also have exactly two opposite charge loose tau leptons, which need to pass electron and muon vetos, and have a MMC combined invariant mass of $75 < m_{tautau}^{\mathrm{MMC}} < 175$ GeV, corresponding to $m_h = 125$ GeV. The large window here compensates for the resolution of the MMC algorithm. Two additional selection conditions are applied after an optimization study performed on different kinematic variables. The first of these is that the tau lepton with highest p_T should have a transverse energy of $E_T > 35$ GeV. Finally, events where the reconstructed di-lepton p_T is smaller than $0.64 \times m_A - 131$ GeV are discarded. This selection is applied to all events with a reconstructed A mass less than 400 GeV.

After the full event selection, the $\tau_{had}\tau_{had}$ analysis has a few surviving background processes, the most prominent of which is the Z+jets background. This background contains jets which are mis-identified as tau leptons. A small contribution from WZ di-boson processes also contributes to the fake background. Other important backgrounds include di-boson ZZ and SM ZH production, which are comprised of true tau signatures, and are estimated from MC. All backgrounds caused by mis-identified jets are estimated via a data-driven template method prediction. This method is performed by constructing three orthogonal control regions. The first region is defined identically to the full signal selection, except that the leading tau is forced to fail the loose tau selection. The second region requires that the tau leptons have the same charge. The third region combines both the inverted loose tau and same tau charge requirements. When looking at data in these regions, the control regions are completely populated by fake tau jets. Data distributions in the control regions are extrapolated into the signal region and used to estimate the mis-identified tau background. The distribution is normalized using m_A sidebands.

Systematic uncertainties due to the fake background normalization are considered by taking into account the fluctuations in normalization values when choosing alternate control regions. This uncertainty constitutes the largest uncertainty, approximately 25%. Uncertainties due to detector calibration effects, and theoretical uncertainties are also included. The m_A distribution of the $\tau_{had}\tau_{had}$ channel after full event selection is given in figure 3, showing the predicted backgrounds, the 340 GeV mass signal signal with a cross section times branching ratio of 50 fb, and the observed data.

4. Results and Conclusions

A binned likelihood ratio test, along with an asymptotic approximation, is used in order to plot the 95% CL upper limits on the cross section times branching ratio of $\ell\ell\tau\tau$. Figure 4 shows the expected and observed upper limits of gluon-fusion $\sigma \times \mathrm{BR}(A \to Zh) \times \mathrm{BR}(h \to \tau\tau)$ for the combined $A \to Zh \to \ell\ell\tau\tau$ analysis. No assumptions are made on the branching ratio of $h \to \tau\tau$ in order to maintain the result model independent. The observed combined upper limit is within 2σ of the expected limit. The expected 95% CL for the $\tau_{lep}\tau_{lep}$, $\tau_{lep}\tau_{had}$ and $\tau_{had}\tau_{had}$ are shown in dashed lines. The drop in the limits at higher values are from the lack of data observed in the highest m_A bins. The 95% CL upper limits on the gluon-fusion $\sigma \times \mathrm{BR}(A \to Zh) \times \mathrm{BR}(h \to \ell\ell\tau\tau)$ range from 0.098–0.013 pb in a range of $220 \leq m_A \leq 1000$ GeV. No excess is observed outside the 2σ. The low observed limits at the higher mass points is caused by a lack of events in the final 315-2000 GeV m_A^{rec} bin.

The final limits are combined with limits from a complementary $A \to Zh \to ffb\bar{b}$ analysis,

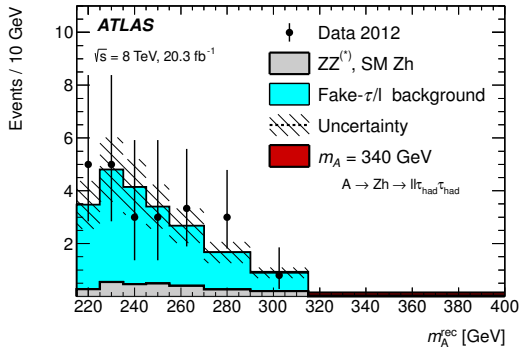

Figure 3. The reconstructed A boson mass, m_A of the $\tau_{had}\tau_{had}$ channel after full event selection [17].

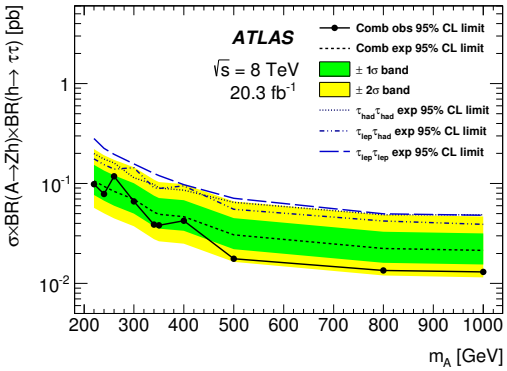

Figure 4. Expected and observed 95% CL upper limits of the gluon-fusion cross section times branching ratio of the combined $A \to Zh \to \ell\ell\tau\tau$ [17].

where $f = \ell, \nu$ [17]. They are interpreted in the context of the four 2HDM scenarios us in order to exclude sections of the phasespace. The final paper includes the first published search for an A boson in the $\ell\ell\tau\tau$ channel.

References

[1] The ATLAS Collaboration 2013 Measurements of Higgs boson production and couplings in diboson final states with the ATLAS detector at the LHC *Phys.Lett. B* **726** 88

[2] CMS Collaboration 2013 Combination of standard model Higgs boson searches and measurements *CMS-PAS-HIG-13-005*

[3] The ATLAS Collaboration 2013 Evidence for the spin-0 nature of the Higgs boson using ATLAS data *Phys.Lett. B* **726** 120

[4] CMS Collaboration 2013 Study of the Mass and Spin-Parity of the Higgs Boson Candidate Via Its Decays to Z Boson Pairs *Phys.Rev.Lett.* **110** 081803

[5] Langacker P 1981 Grand unified theories and proton decays *Phys.Rev.Lett.* **72** 185

[6] Branco G C, *et al.* 2012 Theory and phenomenology of two-Higgs-doublet models *Phys.Rept.* **516** 1

[7] Kim J E 1987 Light Pseudoscalars, Particle Physics and Cosmology *Phys.Rept.* **150** 1

[8] Joyce M, Prokopec T and Turok N 1994 Nonlocal electroweak baryogenesis. Part 2: The Classical regime *Phys.Rev.* **D53** 2958

[9] The ATLAS Collaboration 2013 Beyond-the-Standard-Model Higgs boson searches at a High-Luminosity LHC with ATLAS *ATLAS-PUB-2013-016*

[10] CMS Collaboration 2013 Search for extended Higgs sectors in the H to hh and A to Zh channels in $\sqrt{(s)} = 8$ TeV pp collisions with multileptons and photons final states *CMS-PAS-HIG-13-025*

[11] CMS Collaboration 2014 Search for a pseudoscalar boson A decaying into a Z and an h boson in the llbb final state *CMS-PAS-HIG-14-011*

[12] The ATLAS Collaboration 2014 Search for neutral Higgs bosons of the minimal supersymmetric standard model in pp collisions at $\sqrt{s} = 8$ TeV with the ATLAS detector *J. High Energy Phys.* JHEP11(2014)056

[13] The ATLAS Collaboration 2014 Constraints on New Phenomena via Higgs Coupling Measurements with the ATLAS Detector *ATLAS-CONF-2014-010*

[14] CERN 1999 ATLAS: Detector and physics performance technical design report. Volume 1 *CERN-LHCC-99-14*

[15] Sjostrand T, Mrenna S and Skands P 2006 PYTHIA 6.4 Physics and Manual *JHEP* **0605** 026

[16] Elagin A, Murat P, Pranko A and Safonov A 2011 A New Mass Reconstruction Technique for Resonances Decaying to di-tau *Nucl.Instrum.Meth.* **A654** 481

[17] The ATLAS Collaboration 2015 Search for a CP-odd Higgs boson decaying to Zh in pp collisions at $\sqrt{s} = 8$ TeV with the ATLAS detector *CERN-PH-EP-2015-013*